RSC Advances

COMMUNICATION

View Article Online
View Journal | View Issue



Cite this: *RSC Adv.*, 2014, **4**, 52215

Received 3rd September 2014
Accepted 10th October 2014

DOI: 10.1039/c4ra09724f

www.rsc.org/advances



# Increased chemical reactivity achieved by asymmetrical 'Janus' functionalisation of graphene†

Mark A. Bissett,‡*[a] Yuichiro Takesaki,[b] Masaharu Tsuji[ab] and Hiroki Ago[abc]

Chemical functionalisation is a promising method to tune the electronic structure of graphene, and the two-dimensional structure of graphene enables access to both of its faces for various types of functionalisation. Here, we present the effect of covalent functionalisation on the Raman spectrum in terms of monofacial (one-sided) and bifacial (two-sided) functionalisation using both monolayer and bilayer graphene. Asymmetrical or 'Janus' functionalisation is found to provide significantly increased levels of doping compared to other schemes allowing for control over graphene's electronic structure as well as control over surface functionality.

Chemical functionalisation of graphene is of great interest due to the ability to alter its chemical, physical, and electronic properties.[1,2] As graphene is a two-dimensional (2D) material it is possible to functionalise both faces either symmetrically (same molecule on each face) or asymmetrically (different molecule on each face). Asymmetrical chemical functionalisation of graphene, sometimes referred to as 'Janus' graphene, has been the topic of a variety of theoretical[3–5] and experimental[6,7] studies that investigate the effect of this increased level of functionalisation. By increasing the level of functionalisation by attaching molecules to both available faces, as well as asymmetrically functionalising with differing functionalities, it is possible to tailor the properties of graphene for specific applications such as optoelectronic devices.[3,6,7] Janus functionalisation also allows us to affect the chemical reactivity of the opposing graphene face by altering the topological as well as the electronic structure.[6]

As well as monolayer, chemical functionalisation of bilayer graphene is also of great interest, but has been studied much less than monolayer graphene.[8–11] Bilayer graphene can also be asymmetrically functionalised and this is of particular interest as the different functionalities could be used to apply a bias across the bilayer and generate a band gap.[10,12,13] However, previously it has been observed that bilayer graphene has a decreased chemical reactivity, particularly towards electron transfer mediated diazonium chemistry.[8] Thus increasing the degree of functionalisation and doping that occurs on bilayer graphene would allow for a wider range of possible applications.

Raman spectroscopy is the ideal tool to investigate the chemical functionalisation of graphene as it can detect the presence of covalent bonds, doping, and spatial distribution.[14] For both n- and p-type doping of mono and bi-layer graphene the frequency of the G band will increase due to the non-adiabatic Kohn anomaly.[15] The 2D band frequency of monolayer graphene however will increase for p-type doping but will decrease for n-type doping as shown for electrochemically gated graphene.[15,16] Thus, it is possible to easily determine the degree of doping by comparing the relative position of the G and 2D band. However, for bi-layer graphene the discussion is made more complicated due to the presence of multiple sub-peaks that are each differently affected by chemical doping. Recently, Raman spectroscopy was used to investigate the effect of electrochemical functionalisation of bilayer graphene, and noted that the individual sub peaks that make up the 2D peak in bilayer graphene (denoted $2D_{22}$, $2D_{21}$, $2D_{12}$ and $2D_{11}$) are each affected differently by chemical doping.[11] To fully optimise the performance of bilayer graphene based electronic devices it is therefore necessary to better understand the effect of chemical functionalisation on the Raman spectrum.

In this communication we have functionalised monolayer and bilayer graphene with different aryl diazonium molecules (nitrobenzene diazonium (NBD) and methoxybenzene diazonium (MBD)), as well as bifacially functionalising with differing functional groups. The synthesis of both mono and bilayer

[a]*Institute for Materials Chemistry and Engineering (IMCE), Kyushu University, Fukuoka, 816-8580, Japan. E-mail: mark.bissett@manchester.ac.uk*

[b]*Graduate School of Engineering Sciences, Kyushu University, Fukuoka, 816-8580, Japan*

[c]*PRESTO, Japan Science and Technology Agency (JST), Saitama 332-0012, Japan*

† Electronic supplementary information (ESI) available: Detailed experimental methods, further Raman spectra and maps. See DOI: 10.1039/c4ra09724f

‡ Present address: Faculty of Engineering and Physical Sciences, School of Chemistry, University of Manchester, UK.

graphene was undertaken using atmospheric pressure chemical vapour deposition (CVD) and then functionalised using aqueous solutions of aryl diazonium molecules as demonstrated in Fig. 1, with further detail provided in Fig. SI-1 in the ESI.†

Fig. 2a presents representative Raman spectra for monolayer graphene before functionalisation (pristine) and after functionalisation with NBD (electron withdrawing p-type dopant), MBD (electron donating n-type), and Janus functionalisation (MBD–Graphene–NBD). A schematic showing the structure of each scheme is shown in Fig. SI-1 of the ESI.† The effects of covalent diazonium functionalisation on the Raman spectrum of graphene have been investigated previously and provide a wealth of information regarding the electronic structure.[1,17–20] The typical graphene peaks are labelled; D, G and 2D and the dotted line shows that the 2D peak can be fitted with a single Lorentzian curve, indicating monolayer graphene.[14] Typically the 2D band of pristine CVD grown graphene has a full width at half maximum (FWHM) of approximately 30 $cm^{-1}$,[21] in agreement with our value and this increases with doping or strain.[22] Strain can also affect the Raman spectrum of graphene in several ways that are similar to chemical functionalisation such as altering the frequency of Raman peaks and widths.[18,22] However, it is also possible to distinguish between the effects of strain and chemical doping on graphene by comparing the relative peak positions and widths.[18,23,24] This allows us to exclude strain as the cause of the peak shift we observe and focus on the effect of chemical functionalisation.

After functionalisation with NBD (red spectrum in Fig. 2) several key changes occur to the spectrum; (1) the D band intensity increases due to the formation of $sp^3$ covalent attachment sites, (2) the frequency of both the G and 2D bands increases due to p-type doping, (3) the 2D band intensity decreases due to charge transfer and (4) the width of the G peak decreases while the 2D width increases. When we compare this to the MBD functionalised graphene we see that again the D band intensity has increased and the 2D intensity has decreased, but by much less when compared to the NBD and this is due to the lower reactivity of MBD.[17] As shown in the ESI (Fig. SI-2),† the peak positions of G and 2D bands shifts depending on the type and amount of doping. Due to the electron donating nature of MBD the graphene is n-type doped, leading to a decrease in frequency of the 2D band. This allows us to determine the type of doping based on the shift in Raman peak frequency. Fig. SI-3 in the ESI† plots each of the peak parameters (G and 2D frequency, $I_D/I_G$ and $I_{2D/G}$ ratios) for monolayer graphene, while Fig. SI-4 plots the same parameters for bilayer graphene.

When bifacially functionalised with both NBD and MBD to form Janus graphene we see the largest increase in D band intensity as well as the largest decrease in 2D intensity. This may be expected as we are effectively doubling the number of available covalent attachment sites by functionalising both faces of the graphene. However, when we compare the spectrum from the Janus graphene to the NBD bifacially (symmetrically) functionalised graphene, with the same molecule on both faces, we see a smaller increase in the level of functionalisation and

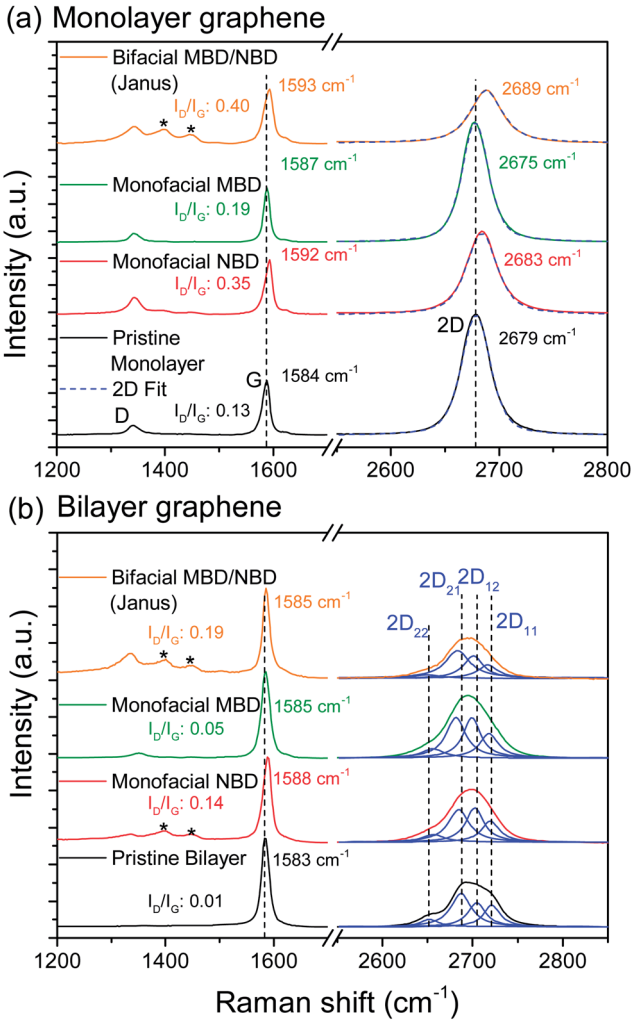


Fig. 2 (a) Representative Raman spectra of pristine monolayer graphene and after functionalisation with NBD, MBD and asymmetrically functionalised with both MBD and MBD to form Janus graphene. The dotted blue line represents the single Lorentzian fit of the 2D peak. (b) Raman spectra for pristine and chemically functionalised bilayer graphene. The 2D peaks are fitted with four Lorentzian components as labelled. (The * indicates aryl diazonium peaks).

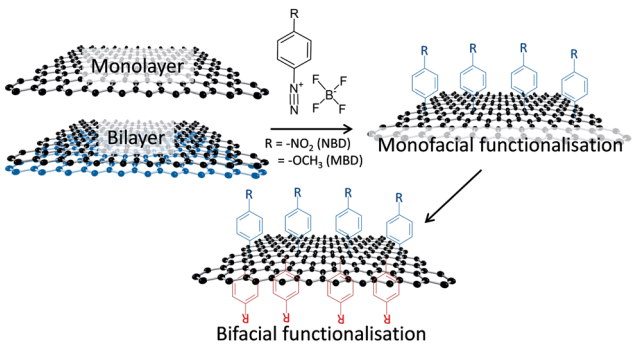


Fig. 1 Schematic showing aryl diazonium functionalisation of mono or bilayer graphene to create monofacial or bifacially functionalised graphene.

doping compared to mono-facial functionalisation. Thus, the increased functionalisation seen in the Janus graphene is caused by more than just the increased number of available reaction sites. This can be explained by considering the effect of doping with the electron donating MBD molecule initially and then functionalising the opposing face with NBD. During diazonium functionalisation the reaction is initialised by an electron transfer from the graphene into the diazonium molecule forming a radical which then subsequently forms the covalent bond to the graphene.[19] By n-type doping one face of the graphene, even only mildly, we have significantly increased the amount of functionalisation possible on the opposing face. The net effect of doping after bifacial functionalisation appears to be p-type, determined from the increased frequency of the 2D band, indicating that the number of NBD molecules far outweighs the MBD molecules. Also it has been shown previously that NBD forms the strongest covalent bond with graphene compared to similar aryl diazonium molecules and that as the density of the attached aryl molecules increases the binding energy can also drastically increase.[25] This demonstrates that it is possible to control the chemical reactivity of graphene simply by functionalising one side with a specific functional group making increased levels of doping possible. Fig. 2b compares the spectra of bilayer graphene before and after functionalisation, with each of the 2D sub peaks fitted. As discussed, bi-layer graphene has a lower reactivity towards diazonium functionalisation and therefore the level of functionalisation is lower when compared to the monolayer graphene. After functionalisation we see the expected changes to the spectrum, such as increased D band intensity and increase in G band frequency. However, the 2D band behaviour is more complex due to the presence of the four different components, as discussed in more detail later.

Previously, the effect of functionalising bilayer graphene with a bromo containing aryl diazonium (BBD) has been investigated.[11] In this previous work they observed that after functionalisation the $2D_{22}$ peak shifted to higher frequencies, while each of the $2D_{21}$, $2D_{12}$ and $2D_{11}$ shifted to lower frequencies.[11] In this work we observed that each of the 2D components increased in frequency after NBD functionalisation. After MBD functionalisation the bilayer spectrum displayed similar behaviour, indicating that the position of the 2D peak components alone cannot be used to differentiate between n- and p-type doping as in the case for single-layer graphene.

In Fig. 3a we can see that the bilayer graphene 2D components positions increase for each functionalisation scheme, although individual components appear to be more sensitive to the doping than others with the $2D_{22}$ showing the largest shift. Interestingly the n-type dopant (MBD) which from the $I_D/I_G$ plot was found to have reacted the least caused the largest shift in 2D component frequency. Previous similar work found that the $2D_{22}$ component frequency increased with doping, but the other three components each decreased slightly.[11] This is slightly different from the results presented here and shown previously for electrically gated bilayer graphene which was found to behave in a similar fashion to monolayer graphene.[15] This different behaviour is attributed to the doping being caused by

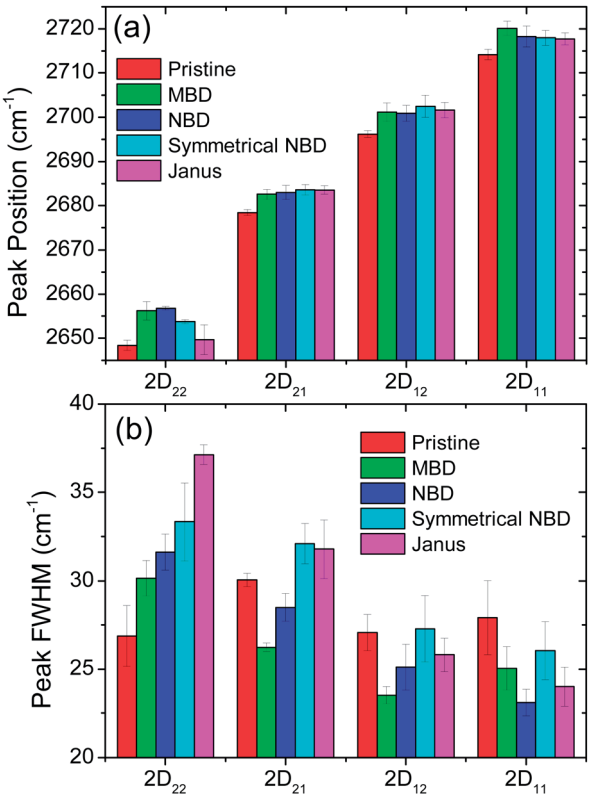


Fig. 3 (a) Column graphs comparing the individual 2D peak component positions ($2D_{22}$, $2D_{21}$, $2D_{12}$ and $2D_{11}$) for bilayer graphene before and after each functionalisation scheme. (b) The FWHM of each of the 2D components. Error bars represent one standard deviation.

the covalent attachment of functional molecules as opposed to an applied external field which will affect each of the graphene layers differently. Fig. 3b compares the FWHM of each of the 2D components, which were found to behave significantly differently after functionalisation and doping. As with peak frequency the $2D_{22}$ components was found to be the most sensitive to the doping, in agreement with previously published results.[11] There is no clear trend with doping type in the FWHM behaviour of the three components ($2D_{21}$, $2D_{12}$ and $2D_{11}$) with both n-type and p-type functionalities causing decreases or increases in the widths. The $2D_{22}$ component however shows a clear increase in width with increasing levels of functionalisation regardless of doping type. This demonstrates that $2D_{22}$ peak width can be reliably used to determine the level and presence of chemical doping in bilayer graphene. It also supports that the Janus functionalisation has significantly larger level of doping than either the monofacial or symmetrically functionalised schemes.

With these high degrees of covalent functionalisation it will be possible to overcome the otherwise prohibitively low reactivity of bilayer graphene and investigate the effect of chemical doping on the electronic structure of bilayer graphene. Also by asymmetrically functionalising with both n-type and p-type functional groups it may be possible to create a bias across the bilayer graphene, which is essential in controlling the electronic structure and integrating into electronic devices.[12] Covalent functionalisation has been shown to greatly affect

both the conductivity and mobility of graphene.[26,27] Typically these results only focus on monofacial functionalisation, however it has been theoretically predicted that bifacial functionalisation can minimise the detrimental disruption to the electrical performance of graphene.[28]

It is also possible to generate Raman maps of chemically functionalised graphene by taking Raman spectra at every point over a large area, allowing us to easily compare the reactivity of differing layers that have each been exposed to identical growth and functionalisation conditions. Fig. 4 shows the Raman map of CVD grown graphene after NBD functionalisation. By mapping the width of the 2D peak (FWHM) we can easily differentiate between the numbers of layers present labelled mono, bi and tri-layer (Fig. 4a). This then allows us to compare the relative reactivity of these layers by plotting the $I_D/I_G$ ratio which is directly proportional to the degree of covalent functionalisation that has occurred. As we can see in Fig. 4b the monolayer area is much more highly functionalised, followed by the bilayer and finally the trilayer area has very little functionalisation. This can also be seen in the representative spectra shown in Fig. 4c, showing the decreasing $I_D/I_G$ ratio with increasing layer number as well as reduced doping. This decreasing reactivity with increasing layer number has been observed before for mechanically exfoliated material and is attributed to decreasing electron transfer rate as the number of layers increases due to shielding from the substrate as well as difference in the graphene morphology.[8,20] Fundamental electrochemical studies have supported this showing increased electron transfer kinetics on monolayer material.[29] As well as electron transfer kinetics, the graphene surface topology can greatly affect reactivity, with rough or strained graphene showing increased reaction rates.[22] It has been shown that monolayer graphene is significantly less flat than multi-layer graphene (bilayer, trilayer) and this can add to the increased reactivity observed of the monolayer graphene.[30,31] Similar trends were observed for each of the functionalisation schemes and further maps can be found in the ESI (Fig. SI-5–7).†

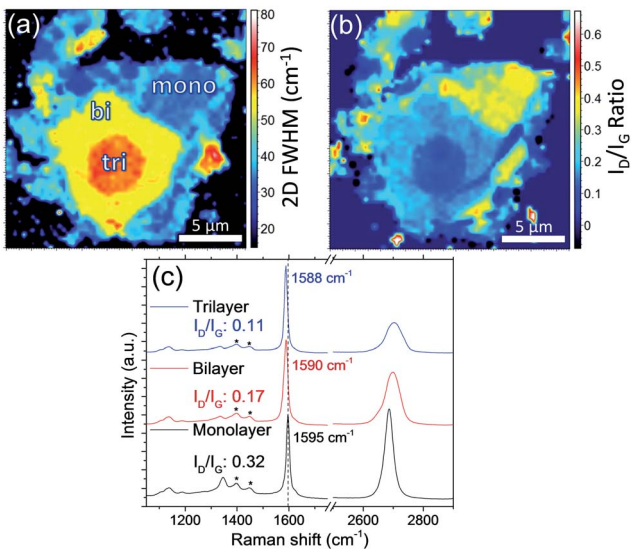


Fig. 4 (a) Raman map of the 2D FWHM of graphene functionalised with NBD. The number of graphene layers is labelled mono, bi and tri. (b) Raman map of the $I_D/I_G$ ratio. (c) Representative Raman spectra from each of the layers. (The * indicates aryl diazonium peaks).

## Conclusions

In summary we have examined the effect of covalent functionalisation with n- and p-type dopants on mono and bilayer graphene and demonstrated how Raman spectroscopy can be used to determine the level of functionalisation in bilayer graphene. We also investigated the effect of bifacial functionalisation to create symmetrically or asymmetrically functionalised (Janus) graphene and the effect on the Raman spectrum. It was found that Janus functionalisation is able to significantly increase the reactivity of the opposing graphene face and produces the highest degree of doping. Through this increased level of functionalisation and doping it may be possible to control the electronic structure of both monolayer and bilayer graphene.

## Acknowledgements

We acknowledge support by PRESTO-JST and the JSPS Funding Program for Next Generation World-Leading Researchers (NEXT Program, GR075).

## Notes and references

1 P. Huang, L. Jing, H. Zhu and X. Gao, *Acc. Chem. Res.*, 2013, **46**, 43–52.
2 H. Liu, Y. Liu and D. Zhu, *J. Mater. Chem.*, 2011, **21**, 3335–3345.
3 M. Yang, R. Zhao, J. Wang, L. Zhang, Q. Xie, Z. Liu and Z. Liu, *J. Appl. Phys.*, 2013, **113**, 084313.
4 Y. Ma, Y. Dai and B. Huang, *J. Phys. Chem. Lett.*, 2013, **4**, 2471–2476.
5 X. F. Chen, Y. Zhu and Q. Jiang, *RSC Adv.*, 2014, **4**, 4146–4154.
6 L. Zhang, J. Yu, M. Yang, Q. Xie, H. Peng and Z. Liu, *Nat. Commun.*, 2013, **4**, 1443.
7 D. Yu, E. Nagelli, R. Naik and L. Dai, *Angew. Chem., Int. Ed.*, 2011, **50**, 6575–6578.
8 F. M. Koehler, A. Jacobsen, K. Ensslin, C. Stampfer and W. J. Stark, *Small*, 2010, **6**, 1125–1130.
9 A. Felten, B. S. Flavel, L. Britnell, A. Eckmann, P. Louette, J.-J. Pireaux, M. Hirtz, R. Krupke and C. Casiraghi, *Small*, 2013, **9**, 631–639.
10 A. J. Samuels and J. D. Carey, *ACS Nano*, 2013, **7**, 2790–2799.
11 Q. H. Wang, C.-J. Shih, G. L. C. Paulus and M. S. Strano, *J. Am. Chem. Soc.*, 2013, **135**, 18866–18875.
12 T. Ohta, A. Bostwick, T. Seyller, K. Horn and E. Rotenberg, *Science*, 2006, **313**, 951–954.
13 T. H. Wang, Y. F. Zhu and Q. Jiang, *J. Phys. Chem. C*, 2013, **117**, 12873–12881.
14 A. C. Ferrari and D. M. Basko, *Nat. Nanotechnol.*, 2013, **8**, 235–246.

 

15 A. Das, B. Chakraborty, S. Piscanec, S. Pisana, A. K. Sood and A. C. Ferrari, *Phys. Rev. B: Condens. Matter Mater. Phys.*, 2009, **79**, 155417.
16 A. Das, S. Pisana, B. Chakraborty, S. Piscanec, S. K. Saha, U. V. Waghmare, K. S. Novoselov, H. R. Krishnamurthy, A. K. Geim, A. C. Ferrari and A. K. Sood, *Nat. Nanotechnol.*, 2008, **3**, 210–215.
17 M. A. Bissett, S. Konabe, S. Okada, M. Tsuji and H. Ago, *ACS Nano*, 2013, **7**, 10335–10343.
18 M. A. Bissett, M. Tsuji and H. Ago, *J. Phys. Chem. C*, 2013, **117**, 3152–3159.
19 G. L. C. Paulus, Q. H. Wang and M. S. Strano, *Acc. Chem. Res.*, 2013, **46**, 160–170.
20 R. Sharma, J. H. Baik, C. J. Perera and M. S. Strano, *Nano Lett.*, 2010, **10**, 398–405.
21 J. D. Wood, S. W. Schmucker, A. S. Lyons, E. Pop and J. W. Lyding, *Nano Lett.*, 2011, **11**, 4547–4554.
22 M. A. Bissett, M. Tsuji and H. Ago, *Phys. Chem. Chem. Phys.*, 2014, **16**, 11124–11138.
23 J. E. Lee, G. Ahn, J. Shim, Y. S. Lee and S. Ryu, *Nat. Commun.*, 2012, **3**, 1024.
24 Y. Kim, D.-H. Cho, S. Ryu and C. Lee, *Carbon*, 2014, **67**, 673–679.
25 P. A. Denis, *ChemPhysChem*, 2013, **14**, 3271–3277.
26 P. Huang, H. Zhu, L. Jing, Y. Zhao and X. Gao, *ACS Nano*, 2011, **5**, 7945–7949.
27 H. Zhang, E. Bekyarova, J.-W. Huang, Z. Zhao, W. Bao, F. Wang, R. C. Haddon and C. N. Lau, *Nano Lett.*, 2011, **11**, 4047–4051.
28 P. Tang, P. Chen, J. Wu, F. Kang, J. Li, A. Rubio and W. Duan, *Nanoscale*, 2013, **5**, 7537–7543.
29 A. T. Valota, I. A. Kinloch, K. S. Novoselov, C. Casiraghi, A. Eckmann, E. W. Hill and R. A. W. Dryfe, *ACS Nano*, 2011, **5**, 8809–8815.
30 V. Geringer, M. Liebmann, T. Echtermeyer, S. Runte, M. Schmidt, R. Rückamp, M. C. Lemme and M. Morgenstern, *Phys. Rev. Lett.*, 2009, **102**, 076102.
31 A. Fasolino, J. H. Los and M. I. Katsnelson, *Nat. Mater.*, 2007, **6**, 858–861.